ELSEVIER

Materials Characterization 58 (2007) 715 – 720

MATERIALS CHARACTERIZATION

Spectroscopic ellipsometry (SE) studies on vacuum-evaporated ZnSe thin films

S. Venkatachalam [a], D. Soundararajan [a], P. Peranantham [a], D. Mangalaraj [a,*], Sa.K. Narayandass [a], S. Velumani [b], P. Schabes-Retchkiman [c]

[a] *Thin film laboratory, Department of Physics, Bharathiar University, Coimbatore - 641046, India*
[b] *Departamento de Fisica, ITESM-Campus, Monterrey, Nuevo Leon, C.P.64849, Mexico*
[c] *Instituto de Física, Univ. Nal. Autónoma de México, A.P.20-364, C.P.01000, Mexico, D.F., Mexico*

Received 27 June 2006; received in revised form 11 October 2006; accepted 16 November 2006

Abstract

Iodine-doped ZnSe thin films were prepared onto well-cleaned glass substrates using vacuum evaporation technique under a vacuum of 3.4×10^{-3} Pa. The composition, structural, optical and electrical properties of the deposited films were analyzed using Rutherford Backscattered Spectrometry (RBS), X-ray diffraction (XRD), spectroscopic ellipsometry (SE) and I–V characteristics. In the RBS analysis, the composition of the deposited film was calculated as $(ZnSe)I_{0.003}$. The structure of the deposited film was identified as cubic, oriented along the (111) direction. The structural parameters such as particle size, strain and dislocation density values were calculated as 28.28 nm, 1.38×10^{-3} lin^{-2} m^{-4} and 1.29×10^{15} lin/m^2, respectively. Spectroscopic Ellipsometric (SE) measurements were done on the $(ZnSe)I_{0.003}$ thin films. The spectral data showed three distinct critical-point structures, including weak structures at $E_0+\Delta_0$, indicating that the sample has a high crystalline quality. The optical band gap value of the deposited films was calculated as 2.63 eV using optical transmittance measurements. From the I–V characteristics studies, the conduction mechanism was found to be SCLC.

Keywords: Thin films; Composition; Structure; Spectroscopic ellipsometry; I–V

1. Introduction

Zinc selenide (ZnSe) is well known as a high refractive index material in multilayer film combinations and as an infrared antireflection coating for solar cells, due to its wide band gap. The growth of II–VI compound semiconductors has attracted considerable attention due to their novel physical properties and wide range of applications in optoelectronic devices. Among these, zinc selenide (ZnSe) material with a direct band gap of 2.7 eV at room temperature, has potential application in light emitting diodes [1] and photoluminescence [2]. In photo-electronic and other properties of the II–VI class of compounds, thin films are highly structure sensitive which in turn can severely influence the device performance. ZnSe film is also used as a buffer layer in thin film solar cells [3]. A broad variety of techniques have been used for the deposition of ZnSe films, such as RF magnetron sputtering [4], metalorganic chemical vapour deposition (MOCVD) [5], molecular beam epitaxy (MBE) [6] and vacuum

* Corresponding author. Tel.: +91 422 2425458; fax: +91 422 2422387.
E-mail address: dmraj800@yahoo.com (D. Mangalaraj).

1044-5803/$ - see front matter © 2006 Elsevier Inc. All rights reserved.
doi:10.1016/j.matchar.2006.11.026

evaporation [7]. ZnSe has either a Sphalerite structure with lattice parameter a=5.6688 Å or a Wurtzite structure with lattice parameters a=3.820 Å and c=6.626 Å [8]. In this paper we report on the composition, structural and optical analysis of vacuum evaporated $(ZnSe)I_{0.003}$ thin films.

2. Experimental

High purity Zn (99.999%), Selenium (99.999%) and Iodine (99.99%) were used to prepare the iodine-doped ZnSe compound. Iodine-doped ZnSe compound was prepared by agitating the evacuated (3.4×10^{-3} Pa) and sealed quartz ampoule containing the above mentioned elements at 875 °C. The prepared compound was light yellow in colour. $(ZnSe)I_{0.003}$ powder was thermally evaporated from a molybdenum boat onto well-cleaned glass substrates under a vacuum of 3.4×10^{-3} Pa. During evaporation, the substrates were maintained at room temperature. The composition of the film deposited onto a glass substrate was studied using Rutherford Backscattered spectrometry. 2 MeV He^{+} ion beam was used for the experiment. Details of the experimental set-up can be found in Ref. [9]. The RBS analysis was performed using a simulation code Rump [10]. Thicknesses of the deposited films were measured by a Multiple Beam Interference (Fizeau fringes) technique [11] and the thickness of the as-deposited film was calculated as 225 nm. The surface morphology of the film was studied by SEM [JEOL, JSM 6400]. Structural analyses of the films were made by X-ray diffractormeter (SCINTAG; USA, Cu K_α radiation at λ=0.541 nm) in the 2θ range 20° to 70°. The optical transmittance spectra were recorded using a UV–VIS-NIR spectrophotometer in the wavelength range from 200–2500 nm.

2.1. Optical properties

The extinction coefficient 'k' at various wavelengths has been calculated using the equation [12]:

$$k = \frac{2.303\log\left(\frac{1}{T}\right)}{4\pi t} \quad (1)$$

where T is the transmittance and t is the thickness of the deposited film. The value of the absorption coefficient (α) can be evaluated from the formula [12]:

$$\alpha = \frac{4\pi k}{\lambda} \quad (2)$$

The relation between α and incident photon energy hν can be written as [13]:

$$\alpha h\nu = C_1(h\nu - E_g^d)^{1/2} \quad (3)$$

$$\alpha h\nu = C_2(h\nu - E_g^i)^2 \quad (4)$$

for direct allowed and indirect allowed transitions, respectively, where C_1 and C_2 are two constants, E_g^d, E_g^i are the direct and indirect band gaps, respectively.

3. Results and discussion

3.1. Composition and surface analysis

The composition of the deposited films was measured using RBS analysis. The RBS spectrum for the as deposited film is shown in Fig. 1. The composition of the deposited films was calculated as $(ZnSe)I_{0.003}$/glass and it was found to be nearly stoichiometric with a negligible iodine concentration. The surface morphology of a deposited film measured by atomic force microscopy (AFM) is shown in Fig. 2. It is observed that the deposited films were having irregular surfaces with some impurity phases.

3.2. Structural analysis

An X-ray diffractogram of a $(ZnSe)I_{0.003}$ film deposited on a glass substrate at room temperature is shown in Fig. 3. It is observed that the XRD pattern of the deposited film shows a more preferred orientation along the (111) plane. The (111) direction is the close-packed direction of the zinc blende structure and the deposited films are polycrystalline having the cubic zinc

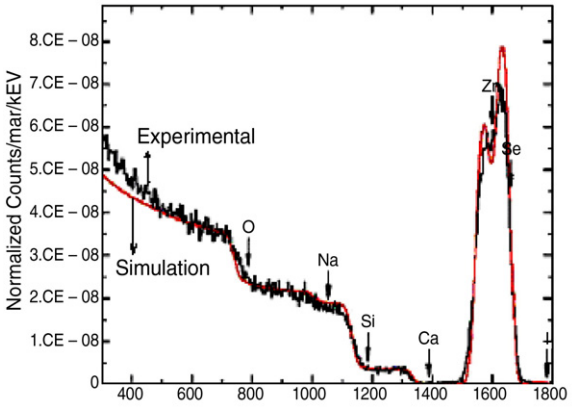

Fig. 1. Rutherford backscattering spectrum of vacuum evaporated $(ZnSe)I_{0.003}$ thin films.

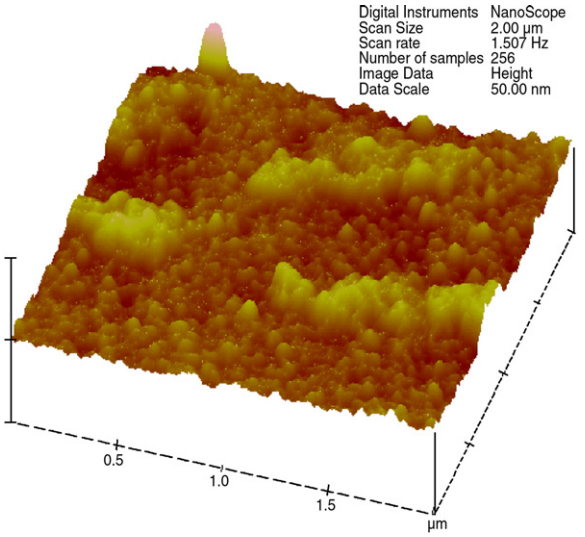

Fig. 2. The surface morphology of the $(ZnSe)I_{0.003}$ thin films deposited onto the glass substrates.

blende structure. The XRD patterns exhibit reflections at $2\theta = 27.21°$, corresponding to the (111) cubic phase [7]. The particle size (D) is calculated using the Scherrer formula from the full width at half maximum (β) [14]:

$$D = \frac{0.94\lambda}{\beta\cos\theta} \tag{5}$$

where λ is the wavelength of the X-rays used, β is the full width at half maximum, D is the particle size value and θ is half the angle between the incident and the scattered X-rays. The dislocation density (δ) can be calculated using the formula [14]:

$$\delta = \frac{1}{D^2} \tag{6}$$

The strain values (ε) can be evaluated by using the following relation [14]:

$$\varepsilon = \left[\frac{1}{D\cos\theta} - \beta\right] \times \frac{1}{\tan\theta} \tag{7}$$

From the above relations, the structural parameters such as particle size (D), strain (ε) and dislocation density (δ) values are calculated as 28.28 nm, 1.38×10^{-3} $\mathrm{lin^{-2}\ m^{-4}}$ and 1.29×10^{15} $\mathrm{lin/m^2}$, respectively.

3.3. Spectroscopic ellipsometry

The ellipsometry angles, ψ and Δ were directly measured by spectroscopic ellipsometry. Fitting three unknown parameters with two measured values, ψ and Δ, carries with it the possibility of ending up with results that lack uniqueness. However, the uniqueness of the results can be fulfilled by using the self-consistency of the Tauc–Lorentz oscillators (via the Kramers–Kroning relationship, Eq. (8)) [15]:

$$\varepsilon_1(E) = 1 + \frac{2}{\pi}\int_0^{\infty} \frac{E''\varepsilon_1(E'')}{E''^2 - E^2}\,dE'' \tag{8}$$

$$\varepsilon_2(E) = \frac{2E}{\pi}\int_0^{\infty} \frac{\varepsilon_1(E'')}{E''^2 - E^2}\,dE'' \tag{9}$$

From the above relations, the value of the pseudodielectric function $\varepsilon(E)=\varepsilon_1(E)+i\varepsilon_2(E)$ is calculated. The values of the real refractive index $n(E)$ and extinction coefficient $k(E)$ are calculated from the following relations [16]:

$$n(E) = \left\{\frac{\left[\varepsilon_1(E)^2 + \varepsilon_2(E)^2\right]^{1/2} + \varepsilon_1(E)}{2}\right\}^{1/2} \tag{10}$$

$$k(E) = \left\{\frac{\left[\varepsilon_1(E)^2 + \varepsilon_2(E)^2\right]^{1/2} - \varepsilon_1(E)}{2}\right\}^{1/2} \tag{11}$$

The absorption edge of ZnSe corresponds to direct transitions from the highest valence band to the lowest conduction band at the Γ point (i.e., $\Gamma_{15}^{V}\rightarrow\Gamma_{1}^{C}$, in single-group notation). The spin-orbit interaction splits the Γ_{15}^{V} valence band into Γ_{8}^{V} and Γ_{7}^{V} (splitting energy,

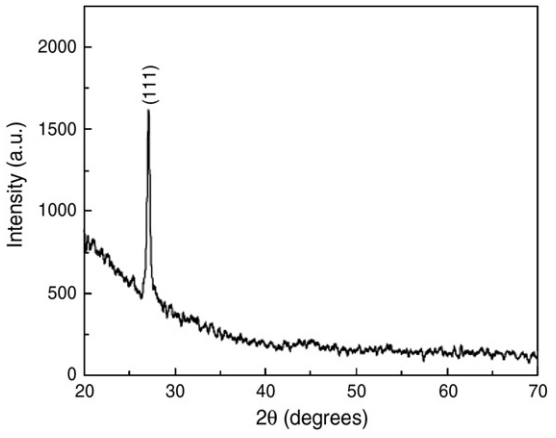

Fig. 3. X-ray diffraction pattern of $(ZnSe)I_{0.003}$ thin films deposited onto glass substrates.

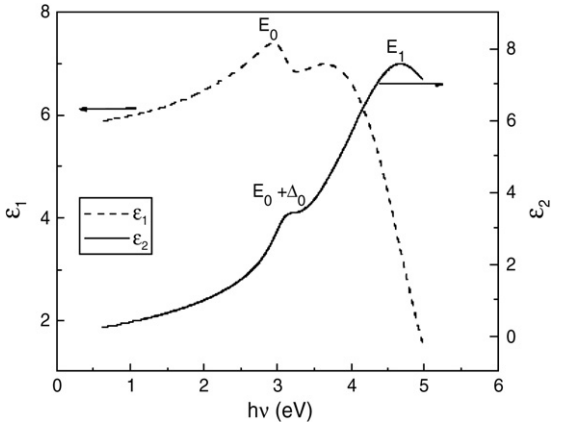

Fig. 4. Spectral dependence of ε_1 and ε_2 of $(ZnSe)I_{0.003}$ thin films.

Δ_0) and the Γ_{15}^C conduction band into Γ_8^C and Γ_7^C (splitting energy, Δ_0^1). The corresponding optical transitions are, respectively labeled $E_0[\Gamma_8^V(\Gamma_{15}^V) \rightarrow \Gamma_6^C(\Gamma_1^C)]$ and $E_0+\Delta_0[\Gamma_7^V(\Gamma_{15}^V) \rightarrow \Gamma_6^C(\Gamma_1^C)]$. The spin-orbit interaction also splits the $L_3^V(\Lambda_3^V)$ valence into $L_{4,5}^V(\Lambda_{4,5}^C)$ and the $L_3^C(\Lambda_3^C)$ conduction band into $L_6^V(\Lambda_6^V)$ and $L_{4,5}^C(\Lambda_{4,5}^C)$, respectively [17]. The corresponding optical transitions are, respectively labeled as $E_1[L_{4,5}^V(L_3^V) \rightarrow L_6^C(L_1^C)$ or $\Lambda_{4,5}^C(\Lambda_3^V) \rightarrow \Lambda_6{}^C(\Lambda_1^C)]$, $E_1+\Delta_1[L_6^V(L_3^V) \rightarrow L_6^C(L_1^V)$ or $\Lambda_6^V(\Lambda_3^V) \rightarrow \Lambda_6^C(\Lambda_1^C)]$ [18]. These points are called critical points (CPs).

The dielectric behaviour of a crystalline material is known to be strongly connected with the energy-band structure. These CP's are associated with transitions in the energy band structure at the energies labeled as E_0, $E_0+\Delta_0$, E_1 and $E_1+\Delta_1$. The E_0 and $E_0+\Delta_0$ transitions are three dimensional (3D) M_oCPs and occur in ZnSe at photon energies ~2.7 eV (E_0) and ~3.1 eV ($E_0+\Delta_0$) at 300 K. The E_1 and $E_1+\Delta_1$ CPs may be of the 3D M_1 type and occur in ZnSe at energies around ~5 eV. In

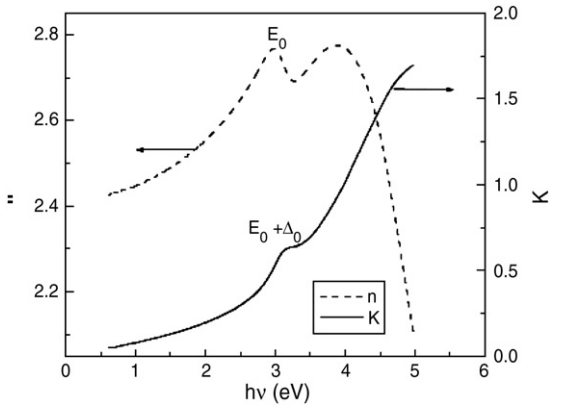

Fig. 5. Numerically calculated spectral dependence of refractive index (n) and extinction coefficient of $(ZnSe)I_{0.003}$ thin films.

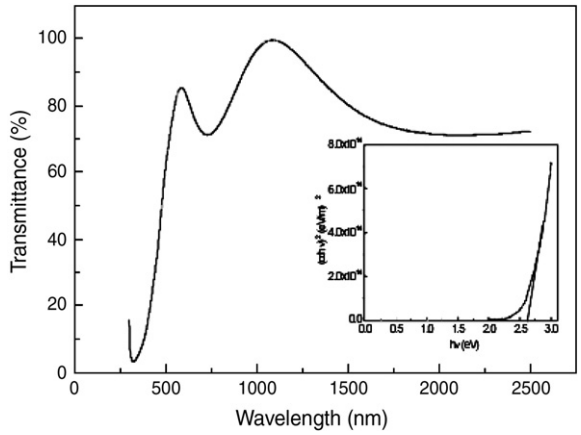

Fig. 6. Transmittance spectrum of $(ZnSe)I_{0.003}$ thin films of 225 nm thickness deposited onto glass substrate.

Fig. 4, we can see clear peaks at 2.93 and 4.72 eV which correspond to 3D M_0 and 3D M_1 type, respectively. These transitions originate from transitions at the E_0 and E_1 edges. Similar results have been reported by earlier investigators [19–21]. Fig. 5 shows the spectral dependence of numerically calculated $n(E)$ and $k(E)$ for $(ZnSe)I_{0.003}$ thin films deposited onto glass substrates.

Similar to ε_1 and ε_2, these spectra reveal the distinct E_0 and $E_0+\Delta_0$ critical-point structures.

3.4. Optical properties

Fig. 6 shows a transmittance spectrum of a (ZnSe) $I_{0.003}$ film deposited at room temperature. This spectrum of the film exhibits a sharp fall of transmittance at the band edge, which confirms that the deposited films have a crystalline nature. This sharp fall of transmittance occurs in the low wavelength region corresponding to

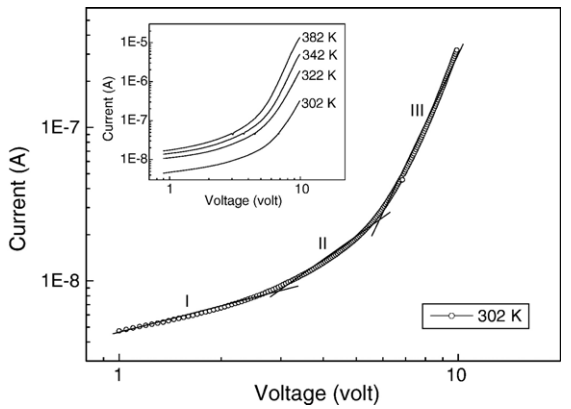

Fig. 7. Current-voltage characteristics of a Al/$(ZnSe)I_{0.003}$/Al sandwich thin film capacitor.

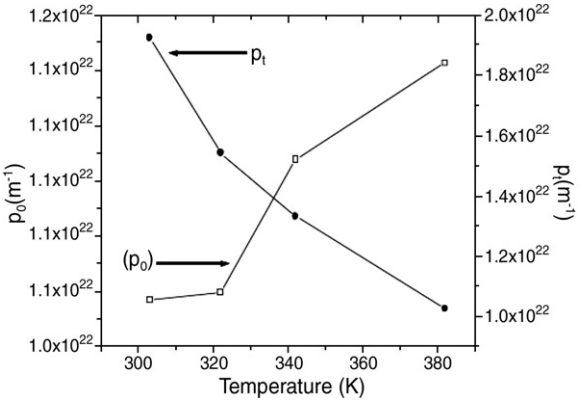

Fig. 8. Plot between the temperature versus p_o and p_t.

the band gap of the film. The inset of Fig. 6 shows a plot between $(\alpha h\nu)^2$ and $h\nu$, which yields the energy gap values of $(ZnSe)I_{0.003}$ films. The energy band gap value of the deposited film is calculated as 2.63 eV. Similar results have been reported by Venkata et al. [22].

3.5. DC conduction studies

The variation of current versus voltage graph of the prepared Al–$(ZnSe)I_{0.003}$–Al device is shown in Fig. 7. In the current versus voltage characteristics, three different types of conduction mechanism were observed. At low voltages (<2.6 V), an Ohmic conduction mechanism is observed. The voltage range between 2.65 to 5.45 V, a trap square law dependence is observed and is very clearly shown in Fig. 7. At higher voltages (>5.5 V), i.e. in the third region for the voltage between 5.5 and 10 V, the current increases rapidly with increasing applied voltage and the slope varies from 3 to 6.43 and is seen to decrease with increasing

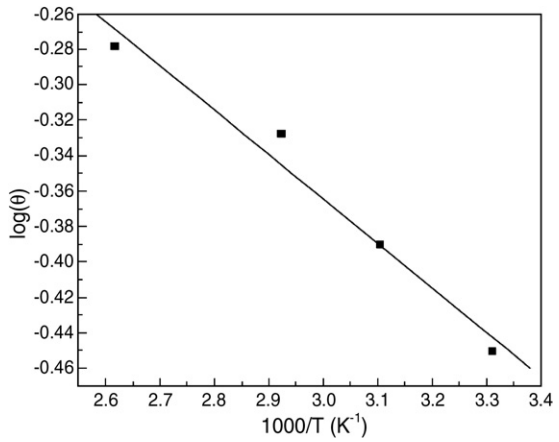

Fig. 9. The graph between θ and inverse absolute temperature.

Table 1
Electrical parameters of $(ZnSe)I_{0.003}$ thin films

T (K)	$\mu \times 10^{-13}$ (m^2/v s)	$p_0 \times 10^{22}$ (m^{-3})	$p_t \times 10^{22}$ (m^{-3})
302	0.389	1.057	1.925
322	0.891	1.060	1.543
342	1.123	1.108	1.332
382	1.306	1.143	1.026

temperature. In the third region, the conduction mechanism is space charge limited (SCLC). The mobility value is calculated from the relation [23]:

$$J = \frac{9}{8}\mu_p \varepsilon' \varepsilon_0 \theta \frac{V^2}{d^3} \tag{12}$$

where μ_p is the hole mobility, ε_0 is the permittivity of free space and ε' is the dielectric constant of the material of the film. The value of trap density (p_t) can be calculated from the relation:

$$\frac{I_1}{I_2} = \theta = \frac{p_0}{p_0 + p_1} \tag{13}$$

The value of free carrier density (p_0) is calculated from the following relation:

$$p_0 = \frac{\varepsilon^1 \varepsilon_0 \theta}{qd^2} V_{tr} \tag{14}$$

The plot between temperature (T) and p_0 and p_t is shown in Fig. 8. The free carrier density (p_0) increases, but the value of trapped carrier density decreases with an increase in temperature. The relation between θ and inverse absolute temperature is shown in Fig. 9. From the slope of the straight line graph, the activation energy has been calculated as 0.251 eV. The calculated values of carrier mobility, free carrier concentration and trap carrier density (p_t) are given in Table 1.

4. Conclusions

The $(ZnSe)I_{0.003}$ thin films were prepared using a vacuum evaporation method. The composition of the deposited film is found to be nearly stoichiometric. In the XRD analysis, the structure of the deposited film is found to be cubic. We have measured the dielectric functions (ε_1 and ε_2) of $(ZnSe)I_{0.003}$ thin films grown on glass substrates using spectroscopic ellipsometry. The spectral data show three distinct critical-point structures, including the weak structures at $E_0 + \Delta_0$, indicating that the sample has a high crystalline quality. The optical studies revealed the existence of direct allowed transitions in the deposited films. A Space charge limited conduction (SCLC) mechanism is observed from the d.c. conduction studies.

References

[1] Tsuguru Shirakawa. Effect of defects on the degradation of ZnSe-based white LEDs. Mater Sci Eng B Solid-State Mater Adv Technol 2002;91–92:470–5.

[2] Gurskii AL, Marko IP, Yuvchenko VN, Yablonskii GP, Hamadeh H, Taudt W, et al. Near-band-edge photoluminescence of MOVPE-grown undoped and nitrogen-doped ZnSe. J Cryst Growth 1997;174:757–62.

[3] Rumberg A, Sommerhalter Ch, Toplak M, Jager-Waldau A, Lux-Steiner MCh. ZnSe thin films grown by chemical vapour deposition for application as buffer layer in CIGSS solar cells. Thin Solid Films 2000;361–362:172–6.

[4] Rizzo A, Tagliente MA, Caneve L, Scaglione S. The influence of the momentum transfer on the structural and optical properties of ZnSe thin films prepared by r.f. magnetron sputtering. Thin Solid Films 2000;368(1):8–14.

[5] Miyajima Takao, Ozawa Masafumi, Asatsuma Tsunenori, Kawai Hiroji, Ikeda Masao. Minority carrier diffusion length in GaN and ZnSe. J Cryst Growth 1998;189–190:768–72.

[6] Wolverson D, Boyce PJ, Townsley CM, Schlichtherle B, Davies JJ. Spin-flip Raman scattering studies of doped epitaxial zinc selenide. J Cryst Growth 1996;159(1–4):229–37.

[7] Kalita Pradip KR, Sarma BK, Das HC. Structural characterization of vacuum evaporated ZnSe thin films. Bull Mater Sci 2000;23(4):313–7.

[8] Joint committee on powder diffraction standards, File No. 9-387 (1990) (XRD).

[9] Jamieson DN. Structural and electrical characterisation of semiconductor materials using a nuclear microprobe. Nucl Instrum Methods Phys Res B Beam Interact Mater Atoms 1998;136–138:1–13.

[10] Doolittle Lawrence R. Algorithms for the rapid simulation of Rutherford backscattering spectra. Nucl Instrum Methods Phys Res B Beam Interact Mater Atoms 1985;9(3):344–51.

[11] Tolansky S. Multiple beam interferometry of surfaces and films. Oxford: Oxford University press; 1948. p. 147.

[12] Venkatachalam S, Mangalaraj D, Narayandass SaK, Kim K, Yi J. Structure, optical and electrical properties of ZnSe thin films. Physica B 2005;358(1–4):27–35.

[13] Prabakar K, Venkatachalam S, Jeyachandran YL, Narayandass SaK, Mangalaraj D. Microstructure, Raman and optical studies on $Cd_{0.6}Zn_{0.4}Te$ thin films. Mater Sci Eng B Solid-State Mater Adv Technol 2004;107(1):99–105.

[14] Venkatachalam S, Rajendra Kumar RT, Mangalaraj D, Narayandass SaK, Kim Kyunghae, Yi Junsin. Optoelectronic properties of $Zn_{0.52}Se_{0.48}$/Si Schottky diodes. Solid-State Electron 2004;48:2219–23.

[15] Harbeke G. In: Abeles F, editor. Optical properties of solids. Amsterdam: North Holland; 1972. p. 21.

[16] Adachi Sadao, Taguchi Tsunemasa. Optical properties of ZnSe. Phys Rev B 1991;43(12):9569–77.

[17] Chelikowsky James R, Cohen Marvin L. Nonlocal pseudopotential calculations for the electronic structure of eleven diamond and zinc-blende semiconductors. Phys Rev B 1976;14:556–82.

[18] Walter John P, Cohen Marvin L, Petroff Y, Balkanski M. Calculated and measured reflectivity of ZnTe and ZnSe. Phys Rev B 1970;1:2661–7.

[19] Kim Young-Dong, Cooper SL, Klein MV, Jonker BT. Optical characterization of pure ZnSe films grown on GaAs. Appl Phys Lett 1993;62(19):2387–9.

[20] Kim Charles C, Sivananthan S. Optical properties of ZnSe and its modeling. Phys Rev B 1996;53:1475–84.

[21] Kvietkova J, Daniel B, Hetterich M, Schubert M, Spemann D. Optical properties of ZnSe and $Zn_{0.87}Mn_{0.13}Se$ epilayers determined by spectroscopic ellipsometry. Thin Solid Films 2004;445–456:228–30.

[22] Venkata YP, Subbaiah P, Prathap M, Devika KT, Ramakrishna Reddy. Close-spaced evaporated ZnSe films: Preparation and characterization. Physica B 2005;365:240–6.

[23] Basol BM, Stafudd DM. Observation of electron traps in electrochemically deposited CdTe films. Solid-State Electron 1981;24:121–5.